Supporting Information (SI) for: Highly active Fe-N_4 sites confined in ordered carbon nanotube arrays as self-supporting cathode catalyst for oxygen conversion

Shuling Liu,[a] Tongjun Li,[a] Guozheng Dong,[a] Xinao Wei,[b] Keke Zhao,[b] Bangan Lu,[c] Yu Chen,[d] Yanyan Liu,*[a,b] Jianchun Jiang,[e] and Baojun Li[a]

[a] College of Chemistry, Zhengzhou University, 100 Science Road, Zhengzhou 450001, P. R. China

[b] College of Science, Henan Agricultural University, 63 Agriculture Road, Zhengzhou 450002, P. R. China

E-mail address: lyylhs180208@163.com (Y.Y. Liu)

[c] College of Materials Science and Engineering, Zhengzhou University, 100 Science Road, Zhengzhou 450001, P. R. China

[d] Key Laboratory of Macromolecular Science of Shaanxi Province, Shaanxi Key Laboratory for Advanced Energy Devices, Shaanxi Engineering Lab for Advanced Energy Technology, School of Materials Science and Engineering, Shaanxi Normal University, Xi'an 710062, P. R. China

[e] Institute of Chemical Industry of Forest Products, Chinese Academy of Forestry (CAF), 16 Suojinwucun, Nanjing 210042, P. R. China

Total number of Fig.s: 16

Total number of tables: 5

Table of Contents

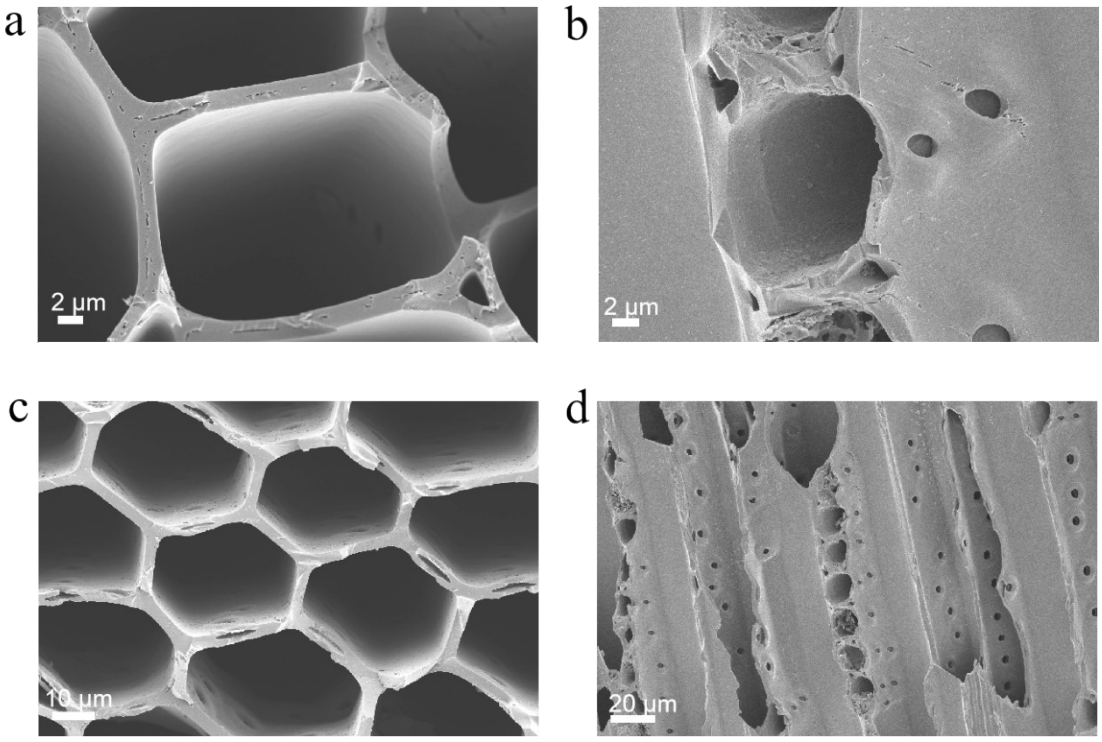

Fig. S1. SEM images of NC at various magnifications through (a) lateral direction and (b) longitudinal direction.

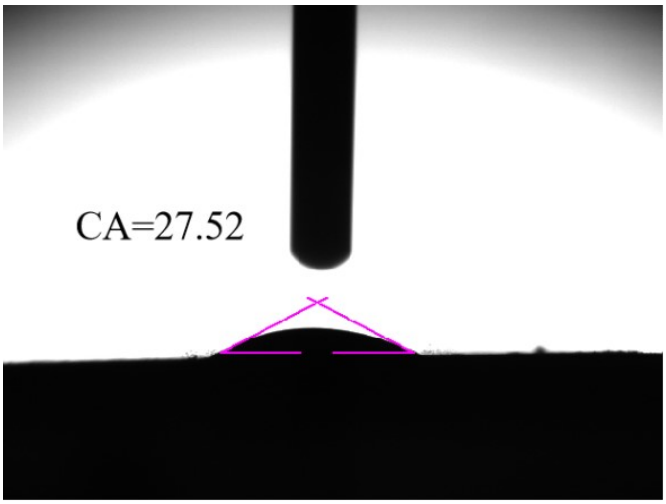

Fig. S2. Contact angle of NC

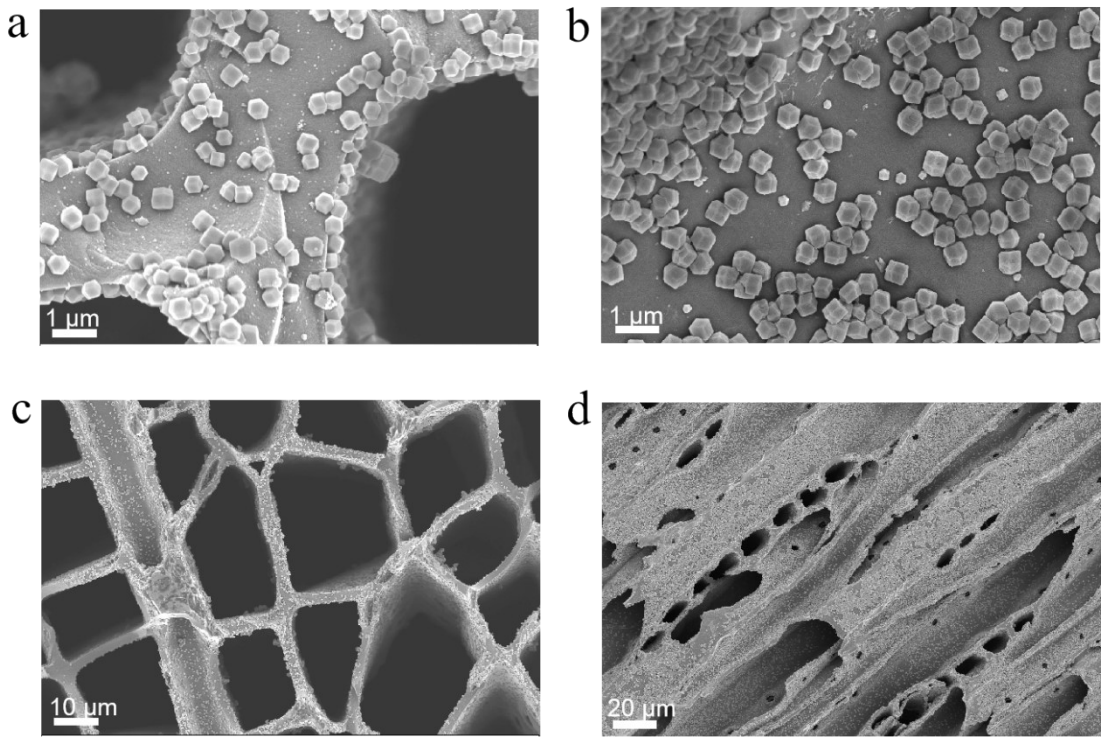

Fig. S3. SEM results of Fe-ZIF-8/NC: (a, c) lateral cutting surface and (b, d) longitudinal cutting surface.

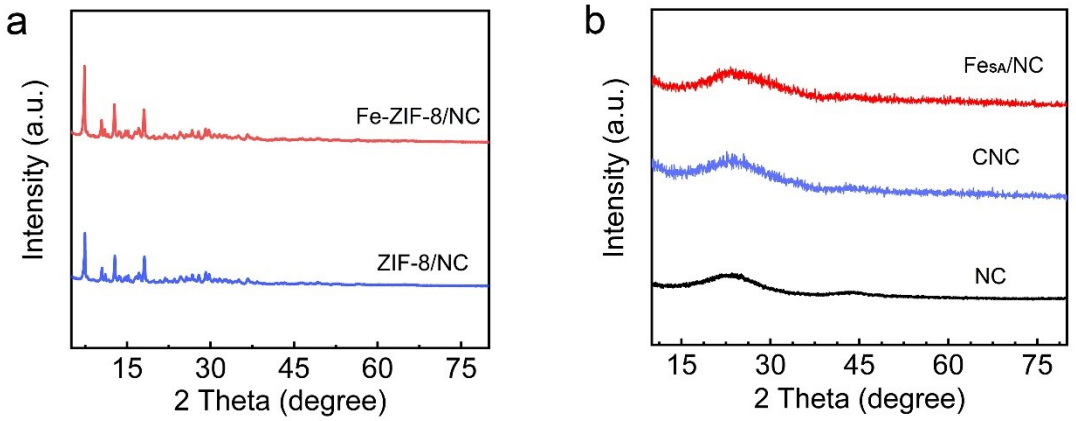

Fig. S4. XRD of (a) Fe-ZIF-8/NC and ZIF-8/NC, (b) Fe_{SA}/NC, CNC and NC.

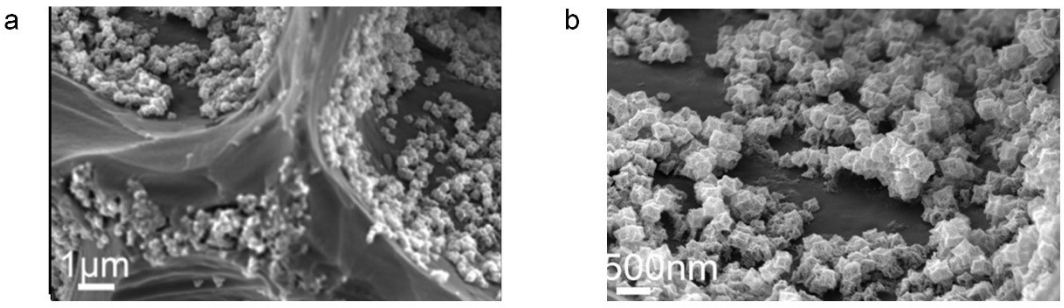

Fig. S5. SEM results of Fe_{SA}/NC.

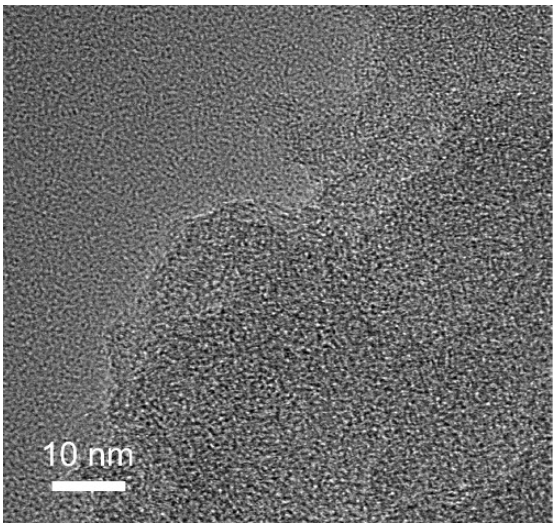

Fig. S6. HRTEM of Fe_{SA}/NC.

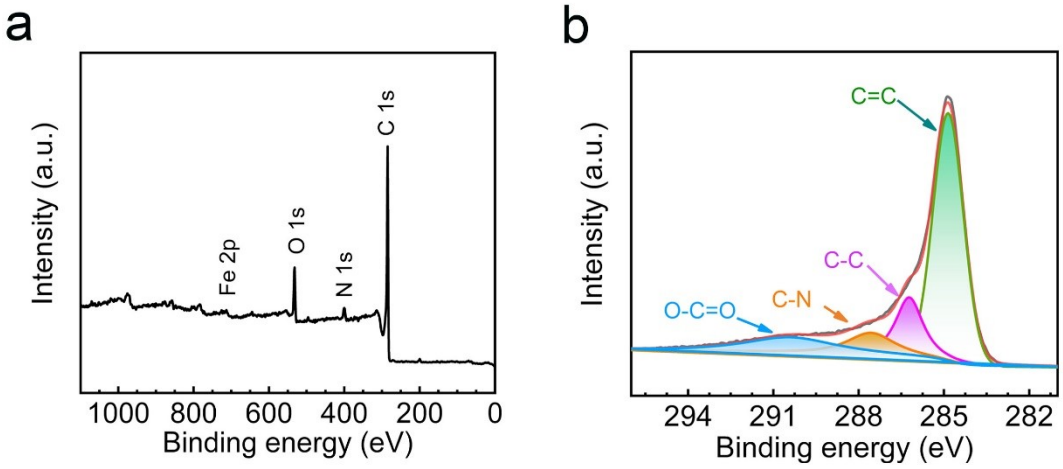

Fig. S7. The XPS spectra of **a** Fe_{SA}/NC, **b** C.

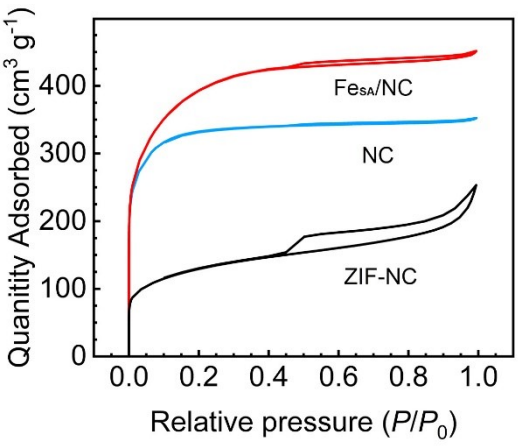

Fig. S8. Nitrogen adsorption–desorption isotherms of Fe_{SA}/NC, ZIF-NC, and NC.

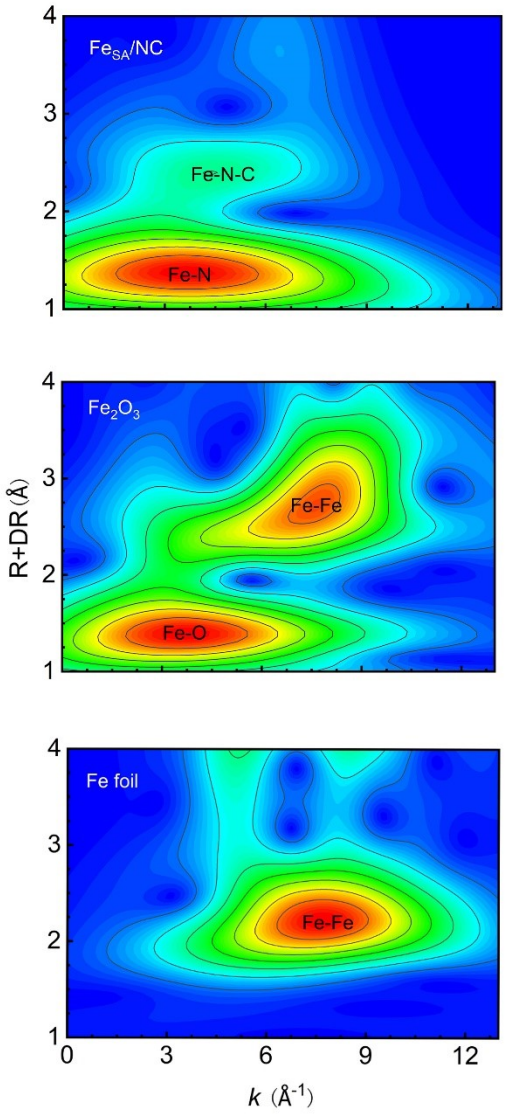

Fig. S9. Wavelet transform (WT) of Fe_{SA}/NC, Fe foil and Fe_2O_3 samples

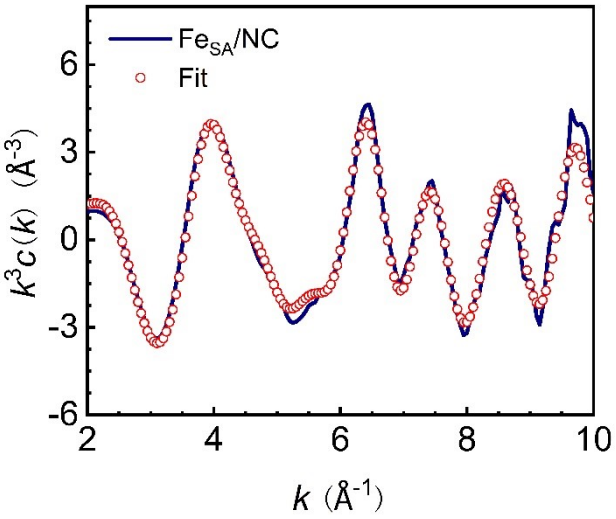

Fig. S10. EXAFS *k*-space fitting curve corresponding to Fe_{SA}/NC

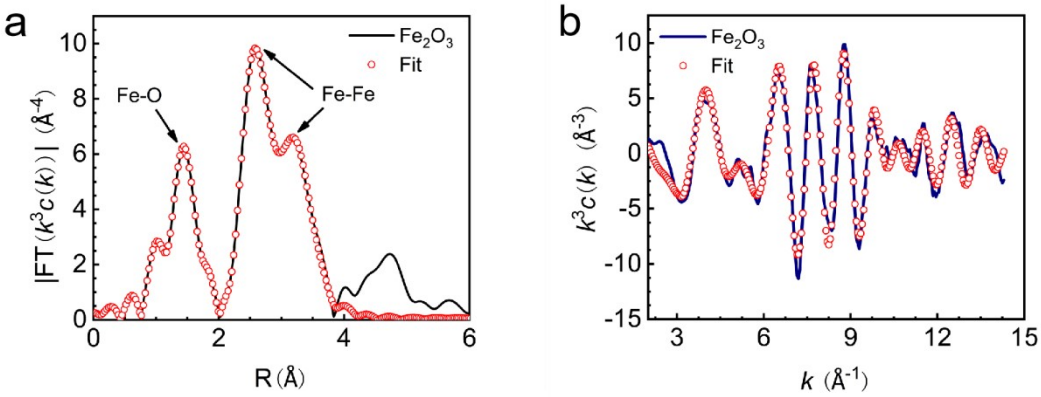

Fig. S11. EXAFS *r*-space and *k*-space fitting curves corresponding to Fe_2O_3.

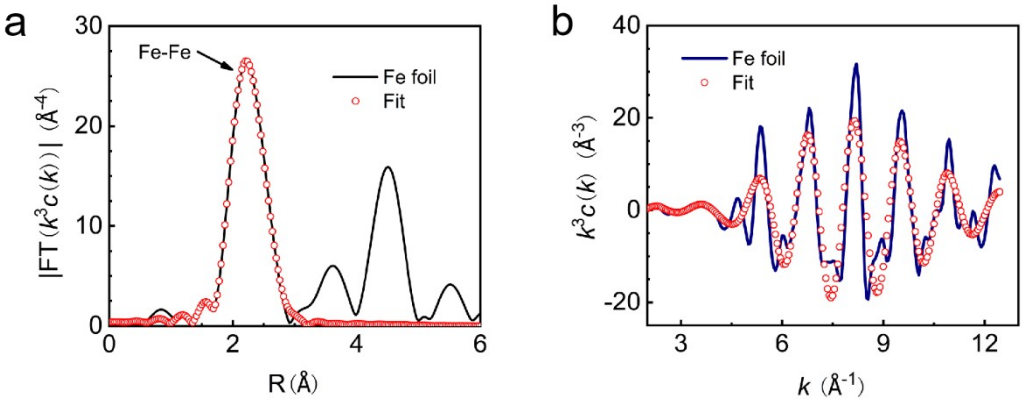

Fig. S12. EXAFS *r*-space and *k*-space fitting curves corresponding to Fe foil.

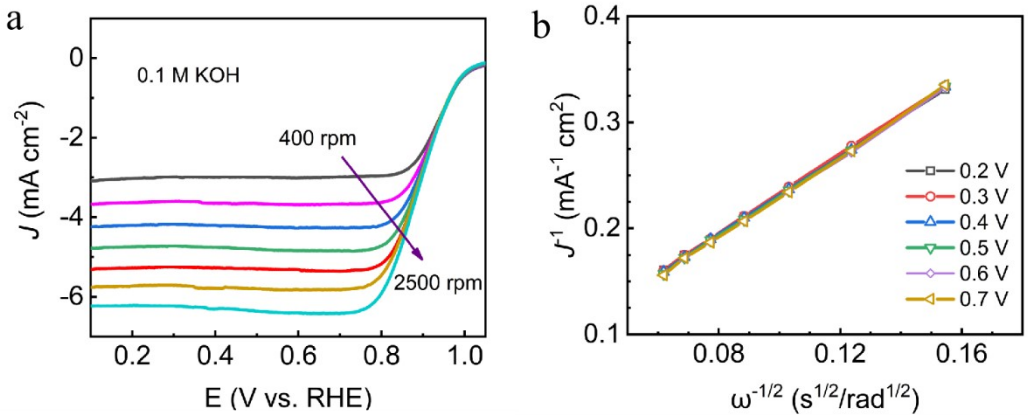

Fig. S13. (a) ORR LSV curves of Fe_{SA}/NC at different rotation rates, (b) the corresponding K-L plots.

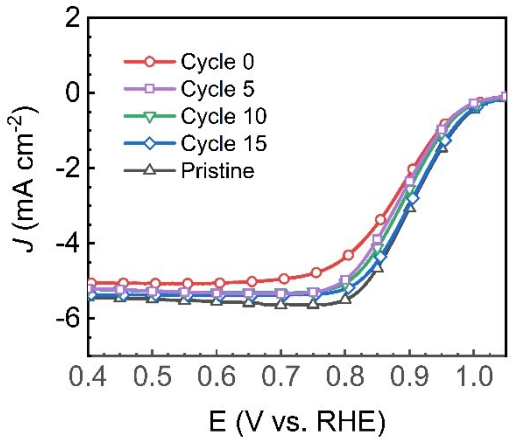

Fig. S14. The results of SCN^- poisoned Fe_{SA}/NC in 0.1 M KOH

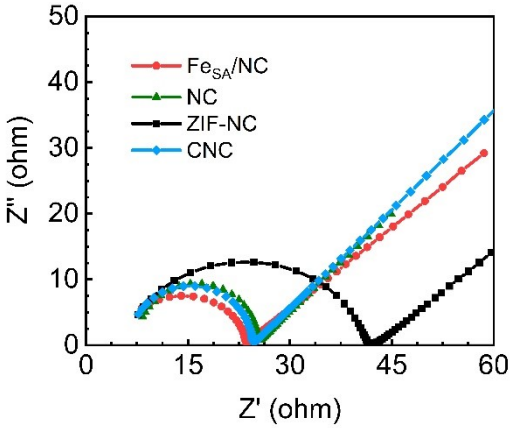

Fig. S15. Impedance diagrams of Fe_{SA}/NC, ZIF-NC, NC and CNC.

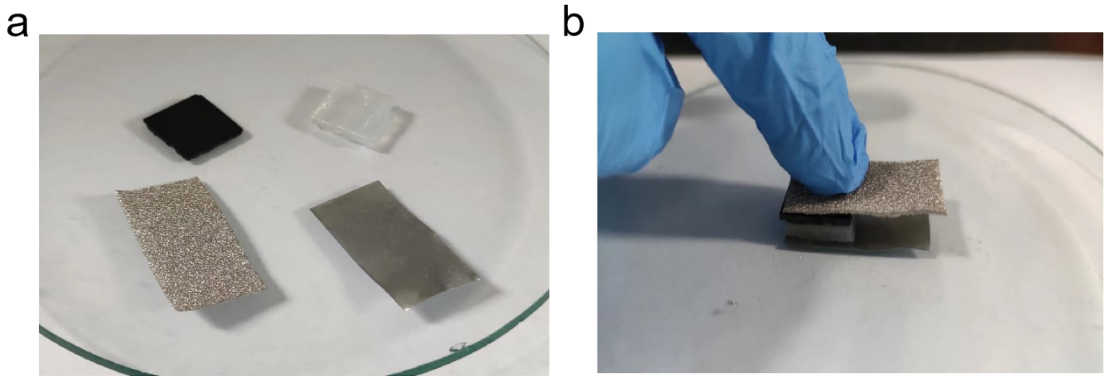

Fig. S16. Fe_{SA}/NC plate-based quasi-solid-state ZAB.

Table S1. Element analysis results of Fe_{SA}/NC determined by XPS and ICP-OES

Catalysts	Fe (wt.%, ICP-OES)	Zn (wt.%, ICP-OES)	Fe	C	N	O
			(at.%, XPS)			
Fe_{SA}/NC	0.95	0.04	0.98	88.23	5.36	5.45

Table S2. BET surface and pore volume of samples.

Sample name	BET surface area (m^2g^{-1})	Total pore volume (cm^3g^{-1})
NC	1229	0.38
Z-NC	453	0.06
Fe_{SA}/NC	1378	0.23

Table S3. EXAFS fitting parameters at the Fe K-edge for various samples

Sample	Shell	*CN*[a]	*R*(Å)[b]	σ^2(Å^2)[c]	ΔE_0(eV)[d]	*R* factor
Fe *K*-edge (S_0^2=0.811)						
Fe foil	Fe-Fe	8*	2.470±0.009	0.0058±0.0019	6.6±1.6	0.0014
	Fe-Fe	6*	2.852±0.009			
Fe_2O_3	Fe-O	5.8±0.9	1.956±0.028	0.0126±0.0038	-0.8±1.7	0.0086
	Fe-Fe	5.2±0.4	2.977±0.017	0.0078±0.0019	1.4±2.7	
	Fe-Fe	5.2±0.7	3.473±0.013			
	Fe-Fe	3.9±0.3	3.717±0.019			
Fe_{SA}/NC	Fe-N	4.6±0.5	1.893±0.009	0.0106±0.0023	-2.5±0.4	0.0016
	Fe-N-C	1.6±0.4	2.961±0.015	0.0156±0.0041	8.7±0.6	

Table S4. Comparison of ORR activity of various non-precious catalysts.

Catalysts	Electrolyte	E_{onset} (V vs. RHE)	$E_{1/2}$ (V vs. RHE)	Data source
Fe_{SA}/NC	0.1 M KOH	1.06	0.90	This work
	0.5 M H_2SO_4		0.80	
Fe/SNCFs-NH_3	0.1 M KOH	1.02	0.89	Adv.Mater.2021, 2105410
SA-Fe/NG	0.1 M KOH	0.99	0.88	Sci. USA 2018, 115, 6626.
Fe–NC–SAC	0.1 M KOH	0.98	0.9	Nat. Commun. 2019, 10, 1278.
Fe-SAC/NC	0.1 M KOH		0.86	Nano Energy 2020, 72, 104670
meso-Fe-N-C	0.1 M KOH		0.846	ACS Catal. 2021, 11, 74-81
Fe/N-CNRs	0.5 M H_2SO_4	0.90	0.73	Adv. Funct. Mater. 2020, 2008085
Fe-N-C HNSs	0.1 M KOH	1.046	0.87	Adv. Mater. 2019, 31, 1806312
FeSA-N-C	0.1 M $HClO_4$		0.78	Angew. Chem. Int. Ed. 2018, 57, 8525-8529
Fe-SAs/NPS-HC	0.1 M KOH	0.970	0.912	Nat. Commun. 2018, 9, 5422
FeSA-N-C	0.1 M $HClO_4$		0.8	Nat. Commun. 2020, 11, 1-7
SA-Fe/NG	0.5 M H_2SO_4		0.80	Proc. Natl. Acad. Sci. 2018, 115, 6626-6631
Fe/N-G-SAC	0.1 M KOH		0.89	Adv. Mater. 2020, 32, 2004900[
Fe–N_x ISAs/GHS	0.1 M KOH		0.87	Adv. Sci. 2019, 6, 1801103
Fe-N/P-C-700	0.1 M KOH	0.941	0.867	J. Am. Chem. Soc. 2020, 142, 2404–2412
Fe-SAs/NSC	0.1 M KOH	1.00	0.87	J. Am. Chem. Soc. 2019, 141, 20118–20126
Fe–N–C	0.1 M KOH	0.965	0.85	Nat. Energy 2021, 6, 834–843

Table S5. Performance comparison between Fe_{SA}/NC-based quasi-solid Zinc-air batteries and other quasi-solid zinc-air batteries previously reported

Catalysts	OCV（V）	Power densities（mW cm^{-2}）	Data sourse
Fe_{SA}/NC	1.47	77.3	This work
Co-CoO_x/N-C NSAs	1.32	20.7	ACS Sustainable Chem. Eng. 2019, 8 (1), 452-459.
V-Co_3O_4	1.39	40.6	ACS Catal. 2021, 11 (13), 8097–8103.
FeCo/Se-CNTLDH + Pt/C	1.40	37.5	Nano Lett. 2021, 21 (5), 2255–2264.
V_2O_3/ MnS/CC	1.40	72	Small 2022, 18 (15), 2104411.
Ni-SAs/HCNFs/ Co-NAs	1.38	57.6	ACS Nano 2022, 16 (9), 15273–15285.
$CoSe_2$-NCNT NSA	1.35	40.6	Nanoscale 2021, 13 (5), 3019–3026.